16th ICAAR LISBOA 2020-2022

16th International Conference on
Alkali-Aggregate Reaction in Concrete
Lisboa | LNEC | Portugal | 31 May - 2 June 2022

http://icaar2020-2022.lnec.pt

Heat flux and dissolution of reactive aggregate powders via isothermal nanocalorimetry

Cody M. Strack [(1)], Shinita M Jordan [(2)], Gordon J. Borne [(3)], Robert D. Moser [(4)]

(1) US Army Engineer R&D Center, Vicksburg, USA, Cody.M.Strack@usace.army.mil

(2) US Army Engineer R&D Center, Vicksburg, USA, Shinita.M.Jordan@usace.army.mil

(3) US Army Engineer R&D Center, Vicksburg, USA, Gordon.J.Borne@usace.army.mil

(4) US Army Engineer R&D Center, Vicksburg, USA, Robert.D.Moser@usace.army.mil

Abstract

Modeling alkali-silica reaction has proved difficult due to the litany of variables and mechanisms at play. This study examined one piece of the puzzle by analyzing the thermodynamics of the early-age reactions that drive ASR. Aggregate powders of highly reactive and non-reactive mineralogies were combined with three alkaline solutions and analyzed via a novel isothermal titration calorimetry method for 24 hours at 50°C. Testing of a highly reactive opal powder in a 1N NaOH solution reliably produced the highest cumulative heat, followed by 1N KOH, with the lowest output being a simulated concrete pore solution; while testing of in the same series with a non-reactive quartz sand evidenced negligible reactivity. Dissolution textures, reductions in powder particle size, measurements of dissolved silica content in testing solutions, and historical expansion studies all correlated well with heat evolution by ASR. The nanocalorimetry approach provides a new means to study ASR thermodynamics and the impacts of environmental variables on ASR mechanisms.

***Keywords**: alkali-silica reaction; ASR; calorimetry; modeling; thermodynamics*

1. INTRODUCTION

The aggregate components of concrete can be susceptible to alkali-silica reaction (ASR); a chemical reaction that feeds on disordered silica phases present in some aggregates. With sufficient moisture and the presence of alkalis in the concrete pore solution, ASR can occur and produce a hydrophilic gel that generates expansive pressures within the concrete, leading to severe damage to the structure due to movement, cracking, and other modes of degradation. Due to the prevalence of concrete, this reaction has been heavily studied since it was discovered in the early 1900s. The ability to generate robust, predictive models that consider the fundamental geochemical and thermodynamics-based mechanisms in ASR, however, is somewhat lacking. This is specifically challenging when trying to understand the dependency of ASR on the environmental variables that drive the reaction [1-3]. Modeling is needed not only to ease research but also to better analyze and predict the potential durability risk of structures and subsequently to better plan to remediate an ongoing structural problem. With a complex reaction that is driven by several competing variables (e.g., aggregate mineralogy, cement chemistry, and environmental conditions), devising accurate mathematical models is difficult [1,3]. A comprehensive model for ASR would fulfill two aspects of understanding the reaction: 1) modeling of the chemical reactions with the kinetics and diffusion processes, and 2) modeling of mechanical damage to the concrete and its constituent portions involving fracture mechanics [1-3]. This study focuses on the first piece of the puzzle through examination of the kinetics of early-age reactions that drive ASR.

In the past, research on potential models concerning ASR was limited by the sheer complexity of the reaction, with empirical and semi-empirical studies of ASR-affected structures driving modelling efforts. These were often at the macroscale; thus, more research within smaller orders of magnitude are needed [2-3]. Due to ASR being a multi-stage process, study of the thermodynamics associated with first stage must occur to enable further calculations. The first stage of ASR is the dissolution of silica on the surface of aggregate particles [1]. Dissolution textures have been documented in ASR studies and implicate it is an early effect of interaction between an alkaline solution and a siliceous material [4-6]. Breakdown of the siliceous material is required for continued ASR, thus discovering related thermodynamic data should be useful.

Isothermal titration calorimetry (ITC) is a technique employed in many branches of science, usually concerning biophysical applications such as cell biology and food chemistry. The technique analyzes heat absorbed or released during a potential reaction, providing accurate measurements of the thermodynamics of molecular interactions [7-11]. With its increased sensitivity on the order of 10s of nJ, nanocalorimetry can even reveal the degradation of particle surfaces quantitatively, providing detail in the solid-liquid transition of particles in an aqueous fluid [10]. This technique, to the author's knowledge, has not been applied to cement-based materials, nor altering the method by executing one singular injection rather than several over the course of the test. This unconventional approach aims to monitor mineral dissolution, an early reaction driving ASR. Additionally, the investigation is supplemented by particle size analysis of the aggregate powders to ascertain textural changes that the material may \ with additional dissolved silica measurements of exposure solutions.

2. MATERIALS AND METHODS

2.1 Materials

The reactive aggregate chosen for this study was Beltane opal, an aggregate that provides the mineralogical ingredients, e.g. disorganized silica, for ASR to readily occur. Beltane opal has been shown to contain reactive components (opal-A, opal-C, tridymite) and fails various ASTM standards that test for reactivity [12-15]. Ottawa Sand was selected to function as a reliable control due to its nonreactivity as an inert quartz sand. The sand is high purity (pure SiO_2) and >99% quartz, used as the standard sand for testing cement and strength of concrete by the American Society for Testing and Materials (ASTM), and has passed reactivity standards such as ASTM C1260 [16-19]. The materials were crushed by a Fritsch Pulverisette 5 at 200rpms and sieved to a #45 (0.2mm) to have ample room within a 5mL ampoule.

2.2 Methods

The aggregates were analyzed via laser diffraction by a Malvern Masterizer 3000 for particle size distribution analysis. DI water as the medium dispersant with quartz used as the refractive index standard. The laser obscuration, the range in which laser diffraction is most accurate, was between 5 and 15 percent and sample amounts ranging from 0.1 grams to 3.3 grams with coarser grains requiring more sample. Some samples were sonicated at no more than 5 percent power to prevent clumping and false reads. The samples ran approximately 6 times to ensure proper repeatability and results are given in micrometers.

The samples were imaged via a FEI Nova NanoSEM 630 field emission variable pressure microscope capable of high-resolution imaging on non-conductive materials. Imaging was performed in low-vacuum mode at pressures of 0.1-0.5 mbar and an accelerating voltage of 15-20 kV. All images were acquired using a backscattered electron detector to improve phase contrast. Scanning electron microscopy (SEM) was performed on the powders before being further subjected to analysis methods to account for potential changes in particle size and texture.

Three aqueous solutions were mixed to submerge the aggregate within during nanocalorimetry. They were chosen to provide similar chemical environments found within concrete and included a 1N NaOH solution, 1N KOH solution, and a simulated concrete pore solution (SCPS) (Table 2.1). The chosen pore solution composition is based on the solution present within the pore space of hydrated cement paste of a typical concrete, more commonly used and studied in corrosion research [20-21]. These were prepared by dissolving NaOH, KOH, and CaOH into 3mL of deionized water. 200 mg. of aggregate powder was placed within a 5mL vial. The instrument titrated 1mL of a 4N solution of NaOH, KOH, or a 4X concentrated version of the SCPS into the cell over a period of 16 minutes and 40 seconds. The pre-wetting of the powders with deionized water was done to minimize heat generated by wetting and associated noise that was found to be harmful to the ITC measurements. The suspensions were lightly stirred at 200 rpm for twenty-four hours. These events occur whilst the ampules are kept at a constant temperature of 50°C. Data was collected by a TA Instruments Nano Isothermal Titration Calorimetry (ITC) instrument and exported to Microsoft Excel. The vessels were meticulously cleaned with isopropanol alcohol between tests. Afterwards, the aggregate powder was filtered 3X with deionized water, dried, imaged via SEM, and analyzed again by laser diffraction for comparison. These procedures were conducted three times per aggregate in the three different chemical solution for a total of 18 trials.

Table 2.1: Composition of compounds in aqueous solutions.

Aqueous Solution	Compound Concentration (g/L)		
	KOH	NaOH	$Ca(OH)_2$
1 N NaOH	-	40.0	-
1 N KOH	56.0	-	-
Simulated Concrete Pore Solution	17.94	5.24	2.4

Exposure solutions were tested following nanocalorimetric measurements to quantify the amount of dissolved silica. The aqueous samples were diluted with ultrapure nitric acid in DI water prior to analysis using a modified EPA Method 6010B using a Perkin Elmer Optima 8300 Inductively Coupled Atomic Emission Spectrometer (ICP-AES). Briefly, a 1.0 mL aliquot of sample was pipetted into 9.0 mL of 2% Optima Grade nitric acid in 15-mL test tubes. The samples were inverted until thoroughly mixed and then a 10 µL aliquot of the diluted sample was pipetted into 9.99 mL of 2% Optima Grade nitric acid in 15-mL test tubes for a final dilution of 1:10,000. The diluted samples were inverted until thoroughly mixed before being placed on the autosampler for analysis. The ICP-AES response was established with a calibration blank and a series of three calibration standards (0.1, 1.0, 10.0 mg/L). Scandium was added in-line prior to sample introduction into the plasma to act as an internal standard and correct for instrumental drift.

Processing of the nanocalorimetric data required some manipulation due to the sensitive nature of the technique. Several thermal effects are associated with the method that can affect evaluations on the heat of mixing [8]. This study found one problematic effect; the substantial difference in temperature between the fluid injected in the ampule and the ampule's set temperature. This causes an artificial rise in the heat signal as fluid enters the cell [8]. The specific device used in this study injects the fluid over a period of 16 minutes and 40 seconds. For clarity, the first 20:00 have been removed from the axes of the presented graphs to isolate the pertinent data. An untouched graph is presented to show this artificial heat spike (Figure 2.1) as an example of how the non-reactive sand powder is used as a baseline to calculate the heat flux from the reactive material. In some cases, the heat derived from this discrepancy is still present within the profiles. Data processing has shown that the effect on cumulative heat is minor.

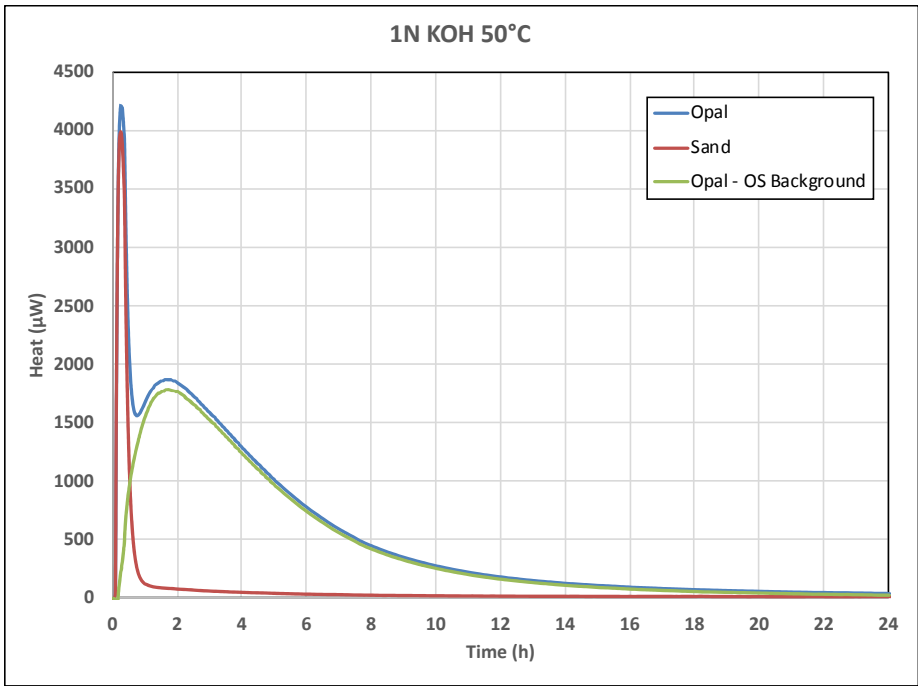

Figure 2.1: Plot of ITC nanocalorimeter analysis of opal and sand. The artificial heat spike is due to injection of fluid into the ampoule. Subtraction of heat associated with an inert material (sand) from a reactive material (opal) can create a heat profile absent of the injection's influence.

3. RESULTS AND DISCUSSION

Analysis of aggregates submerged in 1N NaOH produced three thermal heat flux profiles that despite minor differences in thermal power readings, equate to a similar cumulative heat. The average cumulative heat generated over 24hrs of the three replicate experiments was 221.3 J/g (Figure 3.1). The Ottawa sand behaved predictably inert with recorded heat only responding to the artificial signal generated by injection of the fluid into the vial. Two trials showed essentially the same profile, with minor differences in the initial, artificial heat spike. However, over the course of 24 hours, substantial heat was produced. The two trials generated 38 J/g and 6.1 J/g, respectively (Figure 3.2).

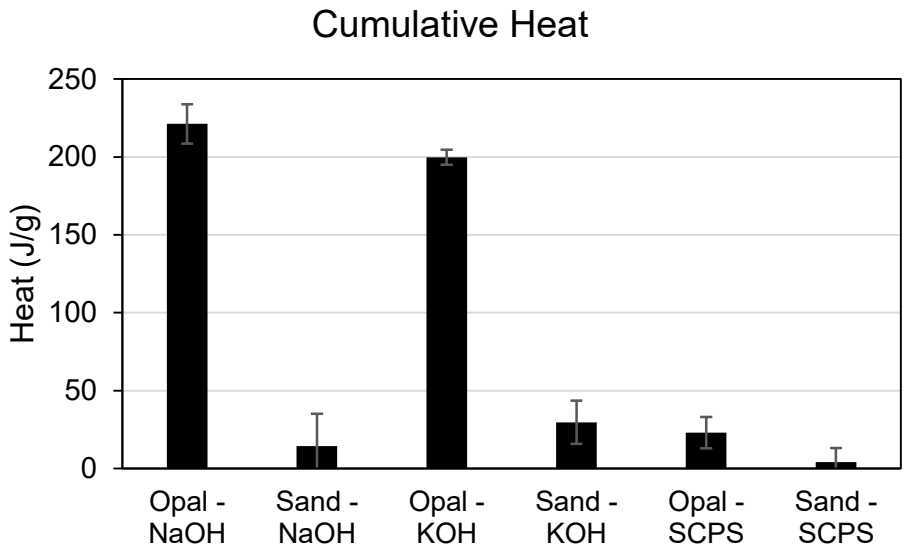

Figure 3.1: Cumulative heat for each aggregate and testing condition.

Similar to the sand's behavior in sodium hydroxide, there were no significant peaks in thermal power generated from the particles' interaction with 1N KOH (heat spike associated with injection not included). Still, with time the analysis showed an average of 30 J/g was generated per trial. Opal was discovered to create heat profiles similar to those in NaOH, albeit at a slightly lesser output. Initial peaks taper off slowly over the course of the 24 hour timeframe resulting in an average cumulative heat of 200 J/g. Analysis of the opal aggregate within SCPS resulted in a lower signal than in the other test conditions. The average cumulative heat of the three trials was 23 J/g. The sand trials showed the lowest heat of the study with cumulative heat of 10 J/g and -2.1 J/g. The latter number may be due to the sensitivity of the instrument as its noisy profile suggests.

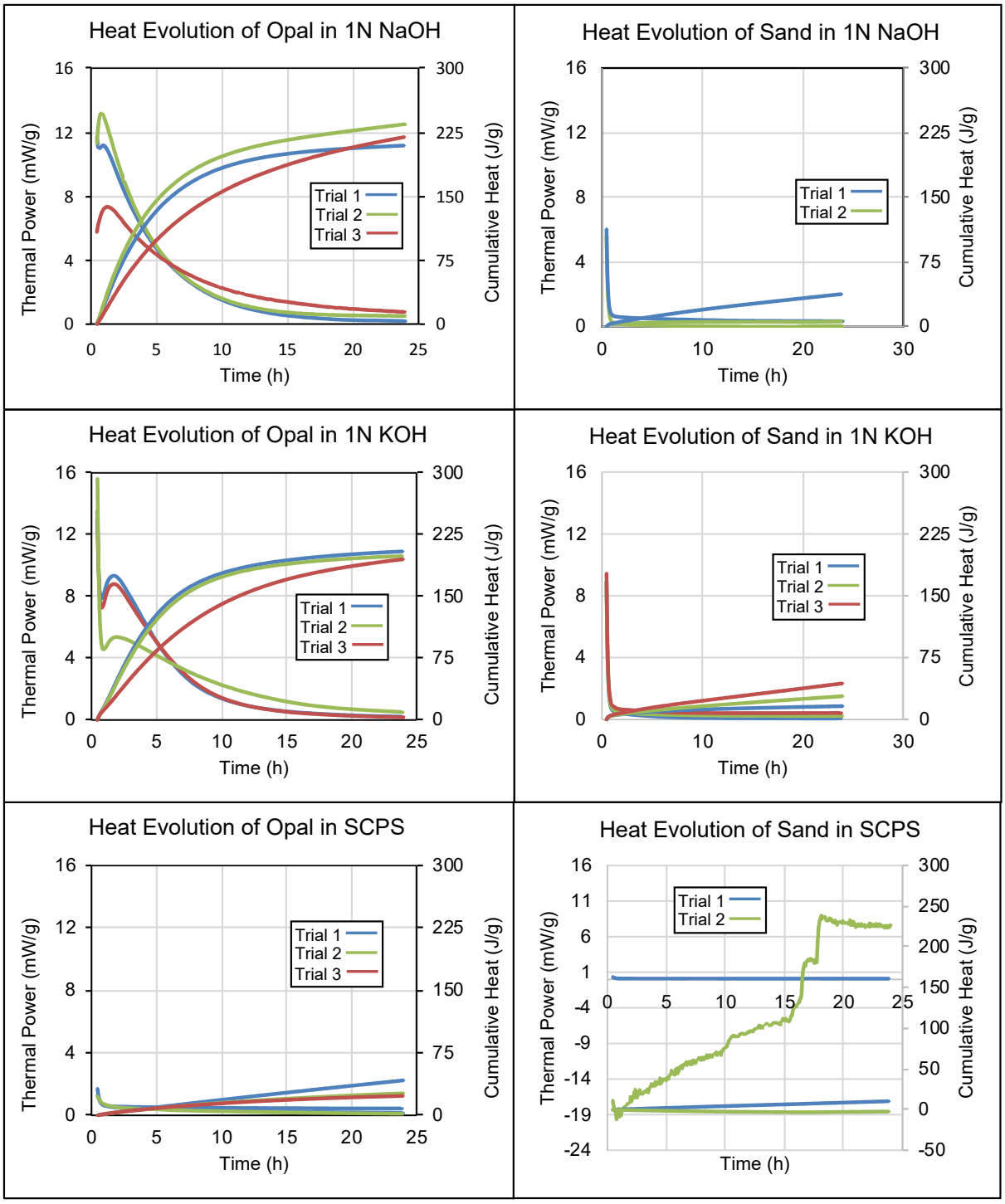

Figure 3.: Heat evolution plots for ITC nanocalorimetry experiments held at a constant temperature of 50C. Multiple trials were conducted per aggregate in three alkaline solutions: 1N NaOH, 1N KOH, and a simulated concrete pore solution (SCPS).

The heat generated within sand trials indicates either there is some reactivity and/or dissolution of the sample within the more caustic solutions (NaOH, KOH) or that due to instrument sensitivity, mixing material in a high temperature setting will result in some exothermic reaction. Despite quartz's stability, dislocations or defects exist within all crystalline solids, providing a pathway to break down the crystal structure [5]. This strain in the crystal lattice could provide the thermodynamic effects needed to explain

a positive cumulative heat [5, 22]. Despite the heat produced, it remains as much as 431% lower than the heat produced during opal experiments.

Analysis of the aggregate powder before and after exposure to the alkaline solutions allows for another avenue to test if the material is reactive. If the particles decrease in size, one can assume they reacted with the alkaline solution, whereas if there is minimal change, one can assume the opposite. The opal saw an 85.2% reduction in average grain size within NaOH, an 80.6% reduction in KOH, and a 49.2% reduction in SCPS. In contrast, the sand saw a 12.1% reduction in average grain size within NaOH, remained unchanged in KOH, and a 17.6% reduction in SCPS (Table 3.1). The high uniformity values for the opal fractions post-test show that a wide range of particle sizes exist and the grains are not all dissolved in an equal way. Preferential dissolution of one grain over another is due to initial grain size, crystal defects, and angularity/sphericity of the particle [5, 22].

Table 3.1: Particle size analysis results of opal and sand aggregates before and after exposure to various alkaline solutions.

	Opal (Pre-Test)	Opal (NaOH)	Opal (KOH)	Opal (SCPS)
Dx (10) (µm)	150	2.87	3.61	14.3
Dx (50) (µm)	252	13.2	23.9	129
Dx (90) (µm)	400	120	130	256
D (4,3) (µm)	262	38.7	50.7	133
Uniformity	0.315	2.473	1.721	0.571
	Sand (Pre-Test)	Sand (NaOH)	Sand (KOH)	Sand (SCPS)
Dx (10) (µm)	161	123	150	56.4
Dx (50) (µm)	255	222	250	212
Dx (90) (µm)	393	366	402	365
D (4,3) (µm)	265	233	265	216
Uniformity	0.281	0.337	0.308	0.415

Electron microscopy of the aggregates reflected the particle size data (Figure 4). Untreated opal particles had crystalline structure and edges, yet after 24 hr within 1N NaOH, the material had nearly dissolved with larger particles (10+ microns) difficult to locate. Similarly, opal in 1N KOH appeared largely broken down with few distinct particles amid the opaline material. After submersion in SCPS, the opal showed dissolution textures, but not overwhelmingly so. Many particles existed that retained their crystalline shape, but displayed a honeycomb texture that is commonly observed in minerals that go through aqueous dissolution [13]. The ability of some grains to resist dissolution whereas others could not can be attributed to the original shape and size of the particles. As Table 3.1 shows, a variety of sizes exists for the sample sets. As the dissolution is of the topochemical type, progress of dissolution would rely on the geometry of the particles [1]. This highlights another complexity in modelling; opal is monomineralic with each surface of a singular grain retaining equal and high reactivity -- ideal circumstances for a model. A realistic system, however, would require establishing constants that account not only for the sphericity and angularity of the grains but also for the varying reactivity of mineral phases present in a singular particle. The sand appeared mostly unchanged in the test conditions; however, some grains were observed with minor pitting. This visual data correlates well with the quantitative particle size data presented in Table 3.1 and assumptions made about the cumulative heat produced.

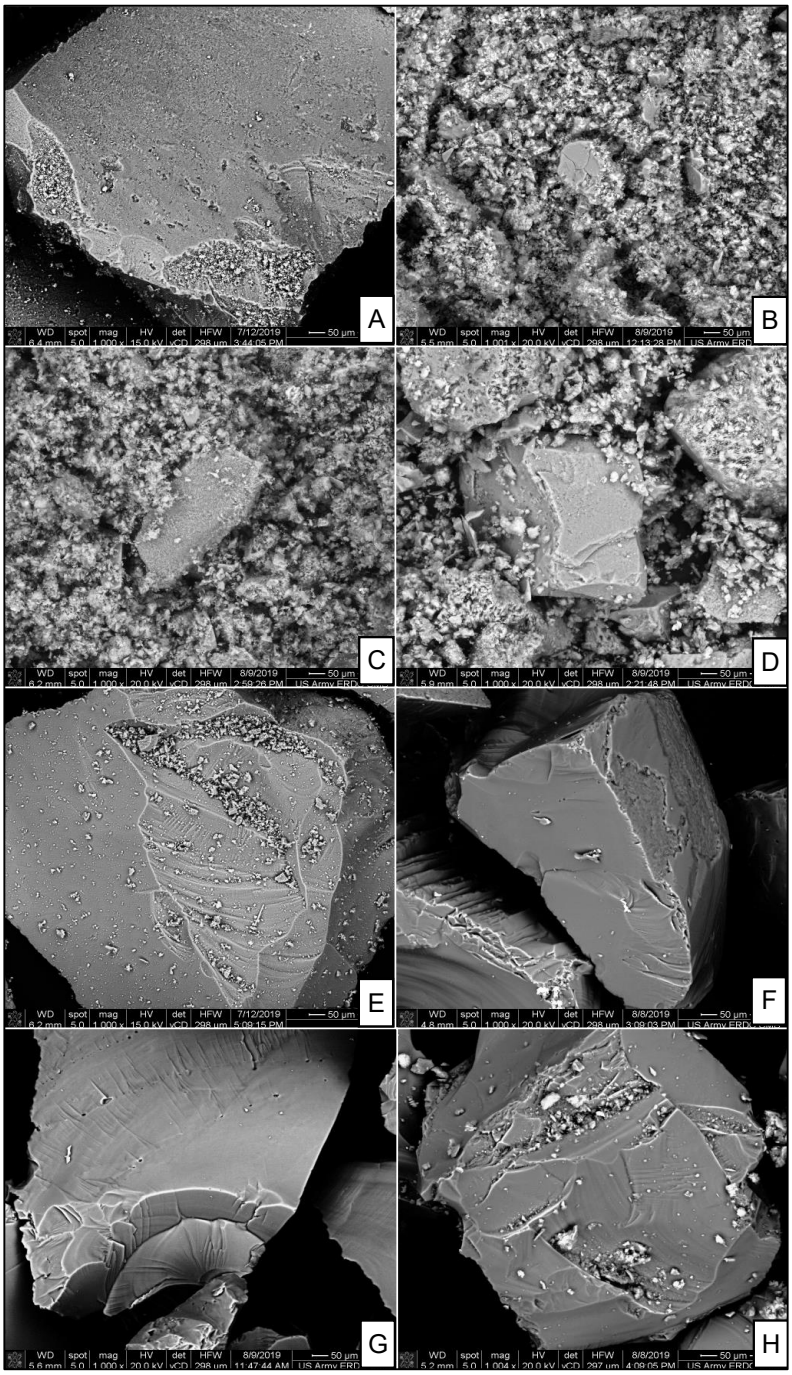

Figure 3.3: SEM images of opal and sand particles under the following conditions: (A) opal, untreated (B) opal, 24 hr in 1N NaOH (C) opal, 24 hr in 1N KOH (D) opal, 24 hr in SCPS (E) sand, untreated (F) sand, 24 hr in 1N NaOH (G) sand, 24 hr in 1N KOH (H) sand.

A final measurement to corroborate the calorimetric, particle sizing, and microscopy results utilized the exposure solutions from the nanocalorimetry experiments to conduct a before-and-after dissolved silica quantification using inductively coupled plasma mass spectroscopy (ICP) methods. The results of this analysis compared with the cumulative heat generation is provided in Figure 3.3. Strong correlation was observed, as in the other measurements, between the reactivity of the aggregate, the heat generated by the ASR process, and the amount of silica dissolved in the solution following nanocalorimetry experiments.

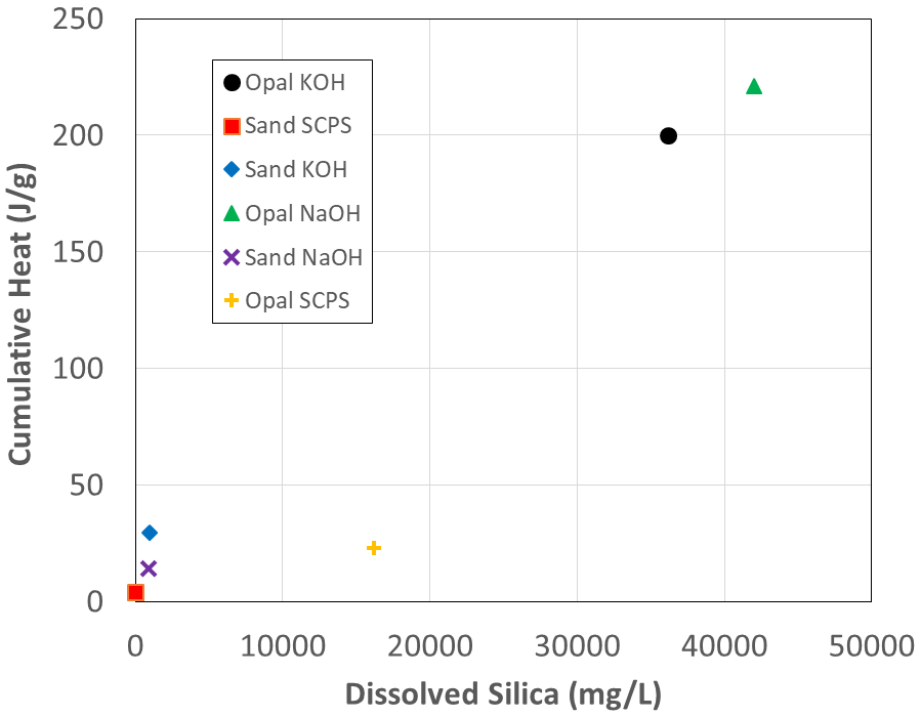

Figure 3.4: Correlation between cumulative heat evolution measured by ICP with dissolved silica measured in exposure solutions.

With many variables at play, several inputs could be altered in future tests to isolate potential effects they may have. The tests reported within this study were held at 50°C as it provided stable, consistent readings. Various temperature regimes could be studied to examine the driving effects of temperature on ASR processes. Many ASR studies have contemplated the role of a pessimum aggregate size with little consensus on what size results in the highest expansion. Physical properties, such as grain size, could be altered to examine how geometries of aggregates affect dissolution. If this experimental method could be used as a screen for aggregate reactivity, it would likely need to be able test aggregates at the same size that would be applied in the field; a potential obstacle for such the capabilities of a nanocalorimeter [2,23]. Lastly, aggregates that are used in real applications, rather than known, highly reactive mineralogies, should be tested to see if and what sort of heat profiles exist for less reactive materials.

4. CONCLUSIONS

- Opal submerged in three alkaline solutions repeatedly produced heat during test conditions of 24 hours held at a constant temperature of 50C. Cumulative heat shows that opal exposed to 1N NaOH produces the most heat, closely followed by 1N KOH. Opal in SCPS produced heat but at smaller amounts, consistent with values exhibited by the control experiments (those with inert quartz sand).
- Textural observations affirm the thermal data. The opal showed dissolution textures with severity correlating with heat produced. The sand had minor occurrences of etched pits, but otherwise did not indicate a substantial reaction with the fluids. Particle size analysis corroborates these finding with a higher cumulative heat correlating with a larger decrease in mean grain size.
- Particle size analysis and corroborates these findings with a higher cumulative heat correlating with a larger decrease in mean grain size. Dissolved silica measurements support these findings as well.
- Thermal data can provide initial inputs regarding thermodynamic modeling of ASR. Steps should be taken to relate these values to current modeling efforts.
- Future research should experiment with temperature sensitivity as this study focused on one temperature regime. Additionally, experiment with other, potentially reactive aggregates as this method has the potential to be a testing plan for reactivity judgments.

5. ACKNOWLEDGEMENTS

This work was conducted under the U.S. Army Engineer Research and Development Center, Geotechnical and Structures Laboratory, United States under contract PE 611102, Project T22 (ASR) products: a study of metastable geomaterial interactions with caustic aqueous media. Permission to publish was granted by Director, Geotechnical and Structures Laboratory.

6. REFERENCES

[1] Bazant ZP, Steffens A (2000) Mathematical model for kinetics of alkali-silica reaction in concrete. Cement Concrete Res 30:419-428.

[2] Rajabipour F, Giannini E, Dunant JH, Ideker M, Thomas DA (2015) Alkali-silica reaction: Current understanding of the reaction mechanisms and the knowledge gaps. Cement Concrete Res 76:130-146.

[3] Pan JW, Feng YT, Wang JT, Sun QC, Zhang CH, Owen DRJ (2012) Modeling of alkali-silica reaction in concrete: a review. Frontiers of Structural and Civil Engineering 6:1-18.

[4] Ponce JM, Batic OR (2006) Different manifestations of the alkali-silica reaction in concrete according to the reaction kinetics of the reactivee aggregate. Cement Concrete Res 36:1148-1156.

[5] Blum AE, Yund RA, Lasaga, AC (1989) The effect of dislocation density on the dissolution rate of quartz. Geochimica et Cosmochimica Acta 54:283-297.

[6] Multon S, Sellier A, Cyr M (2009) Chemo-mechanical modeling for prediction of alkali silica reaction (ASR) expansion. Cement Concrete Res 39:490-500.

[7] Ghai R, Falconer RJ, Collins BM (2011) Applications of isothermal titration calorimetry in pure and applied research – survery of the literature from 2010. Journal of Molecular Recognition 25:32-52.

[8] Rodriguez de Rivera M, Socorro F, Matos JS (2010) Modelling of the thermal effects involvd in determination of heat of mixing using an ITC operating in continuous mode. Journal of Thermal Analytical Calorimetry 99:791-791.

[9] Zhang M, Efremov M Yu, Olson EA, Zhang ZS, Allen LH (2002) Real-time heat capacity measurement during thin-film deposition by scanning nanocalorimetry. Appl Phys Lett 81:3801-3803.

[10] Lai SL, Guo JY, Petrova V, Ramanath G, Allen LH (1996) Size-dependent melting properties of small tin particles: nanocalorimetric measurements. Physical Review Letters 77:99-102.

[11] Freire E, Mayorga OL, Straume M (1990) Isothermal Titration. Analytical Chemistry 62:950-959.

[12] Gutteridge, WA, Hobbs DW (1980) S. Chemical, P.P. Of, B.O. Rock, I.T.S.G. Alkali, S.R. Product, (Communicated by M. Regourd). 10:183–193.

[13] Strack, CM, Barnes E, Ramsey MA, Williams RK, Klaus KL, Moser RD (2020) Impact of aggregate mineralogy and exposure solution on alkali-silica reaction product composition and structure within accelerated test conditions. Constr. Build. Mater. 240.

[14] Shin JH, Struble LJ, Kirkpatrick RJ (2015) Microstructural changes due to alkali-silica reaction during standard mortar test. Materials (Basel). 8:8292–8303.

[15] Kawamura M, Fuwa H (2013) Effects of lithium salts on ASR gel composition and expansion of mortars. Cem. Concr. Res. 33:913–919.

[16] Chiu, YC, Olek J (2014) Using modified mortar-bar test method to access the effects of deicers on expansion of mortars with and without reactive aggregates. Proc. 4th Int. Conf. Durab. Concr. Struct. ICDCS 413–418.

[17] Deschenes, RA, Micah Hale W (2017) Alkali-Silica Reaction in Concrete with Previously Inert Aggregates. J. Perform. Constr. Facil. 31:1–8.

[18] Ojuri, OO, Fijabia DO (2012) Standard sand for geotechnical engineering and geoenvironmental research in Nigeria: Igbokoda sand. Adv. Environ. Res. 4:305-321

[19] Wood SG, Giannini ER, Ramsey MA, Moser RD (2018) Autoclave test parameters for determining alkali-silica reactivity of concrete aggregates. Constr. Build. Mater. 168:683-691

[20] Page CL, Vennesland (1983) Pore solution composition and chloride binding capacity of silica-fume cement pastes. Matériaux Constr. 16:19-25

[21] Poursaee A, Hansson CM (2007) Reinforcing steel passivation in mortar and pore solution. Cem. Concr. Res. 37:1127–1133

[22] Liu M, Yund RA, Tullis J, Topor L, Navrotsky A (1995) Energy associated with dislocations: a calorimetric study using synthetic quartz. Physics and Chemistry of Minerals 22:67-73

[23] Suwito A, Jin W, Xi Y, Meyer C (2002) A mathematical model for the pessimum size effect of ASR in concrete. Concrete Science and Engineering 4:23-34